ORIGINAL PAPER

Sedimentological evidence for the Late Holocene sea level change at the Enjefa Beach exposures of Kuwait, NW Arabian Gulf

Saifullah K. Tanoli

Abstract The mid-late Holocene drop in relative sea level has resulted in the deposition and progradation of coastal facies along the Enjefa Beach in Kuwait, NW Arabian Gulf. These coastal facies display various depositional subenvironments, including landward foreshore beach, tidal channel, shallow tidal channel, and coastal sand flat. The foreshore beach facies consist of dominantly planar laminated beds. Main tidal channel subenvironments are interpreted for the trough cross-bedded facies. The shallow tidal channel deposits are composed of variable oriented planar wedge-shaped and ripple cross-bedded facies. The coastal sand flat deposits consist of extensively burrowed beds with a large network of Ophiomorpha burrows. These exposures are overlain by the recent continental deposits of rubbles and artificial infill. The mere exposed occurrence of these rocks as well as the above facies stacking pattern reflects progradation as a result of relative drop in sea level. Based on the carbon dating of these sediments, the last phase of the relative sea level drop likely occurred around 1,800 years ago. Neotectonics of local structuring, due to the regional northeastward movement of the Arabian Plate under the Zagros Fold Belt, might have a role in this sea receding

Keywords Enjefa Beach · Late Holocene · Sediment

Sea level changes during the last glacial age: an introduction

Variations in sea level are caused by a combination of eustatic, isostatic, and tectonic factors (Anzidei et al. 2011; Lambeck

S. K. Tanoli (✉)
Exploration Studies Team, Exploration Group, Kuwait Oil Company, Ahmadi, Kuwait
e-mail: stanoli@kockw.com

et al. 2011) and the relation between rate of base level change and the sedimentation rate (Catuneanu et al. 2009). Melting of ice after the last ice age of Late Pleistocene has contributed to additional land-locked water to the sea, resulting in an overall sea level rise during the Holocene. The removal of large ice sheets has readjusted the Earth's crust due to change in gravitational potential in higher latitudes (Lambeck 1996). This phenomenon of unloading the melted ice sheets from the earth's crust and adding more melt water weight to the ocean floor results in readjustment of the crust which is named glacio-hydro-isostatic adjustment (Lambeck et al. 1995). However, tectonics and also rate of sedimentation in some areas may accentuate or neutralize the eustatic–isostatic effects locally, adding to spatial variability in sea level. Since the last glacial maximum around 18,000 years ago, as a consequence of melting of the ice sheets, unlocked water resulted in sea level rise. Generally, this sea level rise was initially fast, slowing to very slow afterward from around 7,000 years BP (Fig. 1).

Prior to this global sea level rise, it is widely recognized that the Arabian Gulf was a dry valley (Lambeck 1996) through which the Euphrates–Tigris Rivers flowed (McIntosh 2005) and their deltas might have emptied into the Gulf of Oman (Biot report #422 2007) (Figs. 2 and 3). The present average depth of the Gulf is around 46 m (150 ft), with maximum depth around 82 m (270 ft) (Biot report #422, 2007). From the glaciation peak until 14,000 years BP, the Gulf was free of marine influence (Lambeck 1996). Around 14,000 years BP, the Strait of Hormuz opened as a narrow waterway, and by 12,500 years BP, the central basin had started experiencing marine incursion (Lambeck 1996). The sea transgressed at an average rate of 100–120 m per year across the floor of Arabian Gulf (Sarnthein 1972), based on estimates of the distance covered by the transgressed waters from the Strait of Hormuz to the mouth of the
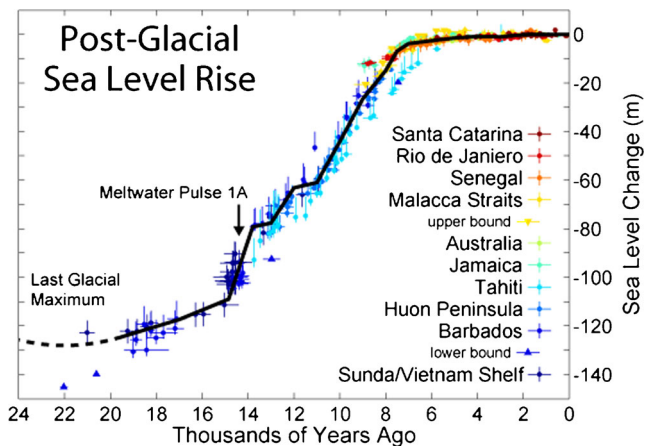
Fig. 1 Change in sea level during the Holocene since the last glacial maxima (the image was created by Robert A. Rohde from published data and was incorporated into the Global Warming Art project)

Euphrates–Tigris. Transgression over this distance, about 1,000 km, took approximately 7,000 years, between 13,000 and 6,000 years BP. Kassler (1973) has suggested fluctuating sea level rise in the gulf floor with relatively rapid rises occurring between 12,000 and 11,000 years BP, 9,500–8,500 years BP, and around 7,000 years BP. The Holocene sea level peaked at around 5,500 years ago and stood about 1–2 m (3–7 ft) higher than the present level in the southern Arabian Gulf (Williams and Walkden 2002). However, Evans et al. (2002) from their study in coastal Abu Dhabi put the peak transgression time around 4,500 years BP, and similarly Evans (2011), put it around 5,000–4,000 years BP. The sea level stood about 3 m (10 ft) higher than the present-day level in the northern Gulf (SEMP, Biot report 422 2007), resulting in sea incursion within the hinterland of

southern Iraq up to Amara and Nasiriyya cities, some 200 km north of the current shorelines of Iraq and Kuwait (Aqrawi 1995). In eastern Saudi Arabia, Holocene deposits close to the shoreline are 3 m (10 ft) higher than the present-day high-water mark (McClure and Vita-Finzi 1982). Carbon-14 isotope age dating of the mollusk shells has yielded an age of 3,700–6,000 years BP for these deposits, confirming this sea level high.

Aqrawi (2001), from his study of Tigris–Euphrates deltaic deposits, concluded that wet climate conditions prevailed due to this transgression to around 6,000 years BP, semi-arid during the regression between 6,000–4,000 years BP, and arid conditions since around 3,000 years BP until present. Similar transgressive coastal brackish marine organic-rich deposits are reported from Bubiyan Island, ca. 8,000 years BP, from North Kuwait (Al-Zamel 1983). These together can be correlated with reported samples around the world by Godwin et al. (1958) for the period 6,000–10,000 years BP.

The Enjefa Beach exposures

The Enjefa Beach exposures lie on the NW shorelines of the Arabian Gulf, within the greater Kuwait city area, in the district of Salwa (Fig. 4). The exposures are in the form of cliff face which is cut by waves and currents and run for about 300–400 m along the north–south beach axis at Enjefa area. The exposure is about 1.6–1.7 m (5–6 ft) in south and 2 to 2.5 m (6–8 ft) in north end above the high-tide mark. Middle part of the studied exposures, which is dominated by trough cross-bedded channel facies, extends seaward in the

Fig. 2 Arabian Gulf Portrayal circa 14,000 years BP when it was a river valley before seawater transgressed through Gulf of Oman (modified from Biot Report #422, original adaptation by M. O'Leary (2007) of map by Nutzel (1979))
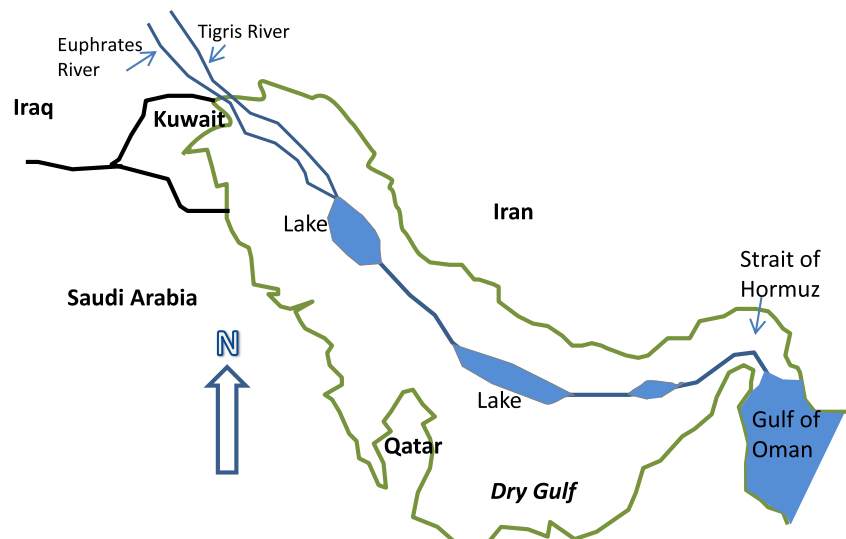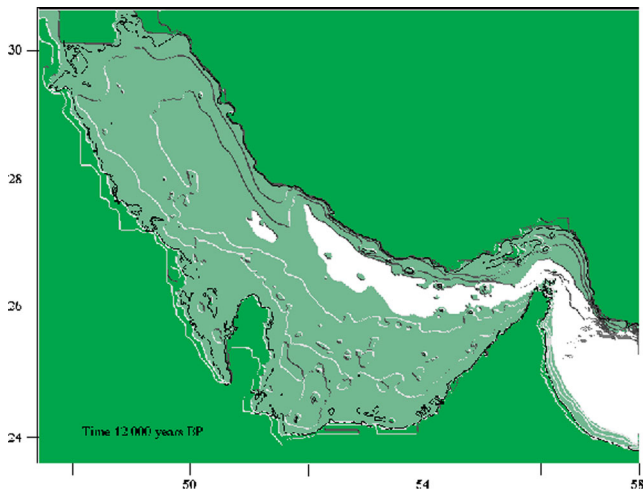
Fig. 3 Reconstruction of the paleo-shorelines and paleo-bathymetry for the Persian Gulf 12,000 years ago. The lower part of the Gulf is first flooded at about 13,000 years BP, but large freshwater lakes could have developed in several locations within the valley floor. Large shallow depressions also occur on the southern margin of the present gulf (Lambeck et al. 1995)

intertidal area as well. The Enjefa Beach is public area and is readily accessible. One can walk alongside the cliff on the beach, which runs parallel to the rock strike, allowing detailed vertical and lateral sedimentological observations, making subenvironments easily discernable.

Four distinct facies can be recognized across the cliff from South toward North:

1. Planar laminated facies
2. Trough cross-bedded facies
3. Planar wedge-shaped and ripple cross-bedded facies, and
4. Bioturbated facies

1. Planar laminated facies

This facies is best exposed along the beach cliff on southern side of the exposures. It occurs as beds made up of thin planar laminae (Fig. 5a). Some beds are around 0.15 m (0.5 ft) thick and consist of very fine sandy to coarse pebbly grains. The coarser parts of the beds are made of bioclasts of clams and oysters, along with pebbles of quartzite and of various igneous rocks. Some of these beds are coarsening upward (Fig. 5b). Thin (mm–cm thick) sharp-based, with generally fining upward trend, white coquina layers are prominent (Fig. 5d). One of the sharp-based and internally cross-bedded coquina beds observed consists of barnacles, clams, and oyster shells, ranging up to 6 cm in thickness (Fig. 5c, d). Within this facies, there are some laterally pinching beds with internal cross-beds, some of which are oriented in opposite direction (Figs. 6 and 7).

This facies is interpreted as a deposit of foreshore beach conditions. The planar lamination was created under upper flow regime conditions in the swash zone (cf. Plint 2010; compare with his Figs. 2 and 28). The coarse upper part of the beds may reflect successive paleo-coastal lines. Similar sediment patterns can also be observed in the present-day beach environments in the vicinity of the study area. However, sharp-based beds such as the coquina bed described above (Fig. 5c, d) depict higher than normal energy events, possibly a storm, which eroded and winnowed the shells before deposition. With waning energy, fining upward sequences develop (cf. Aigner 1985). The same is the case with the fining upward laminae, the only difference being the degree in terms of energy of the event. Laterally pinching beds were deposited in small channels, which were created by the strong currents at least partially associated with tides.

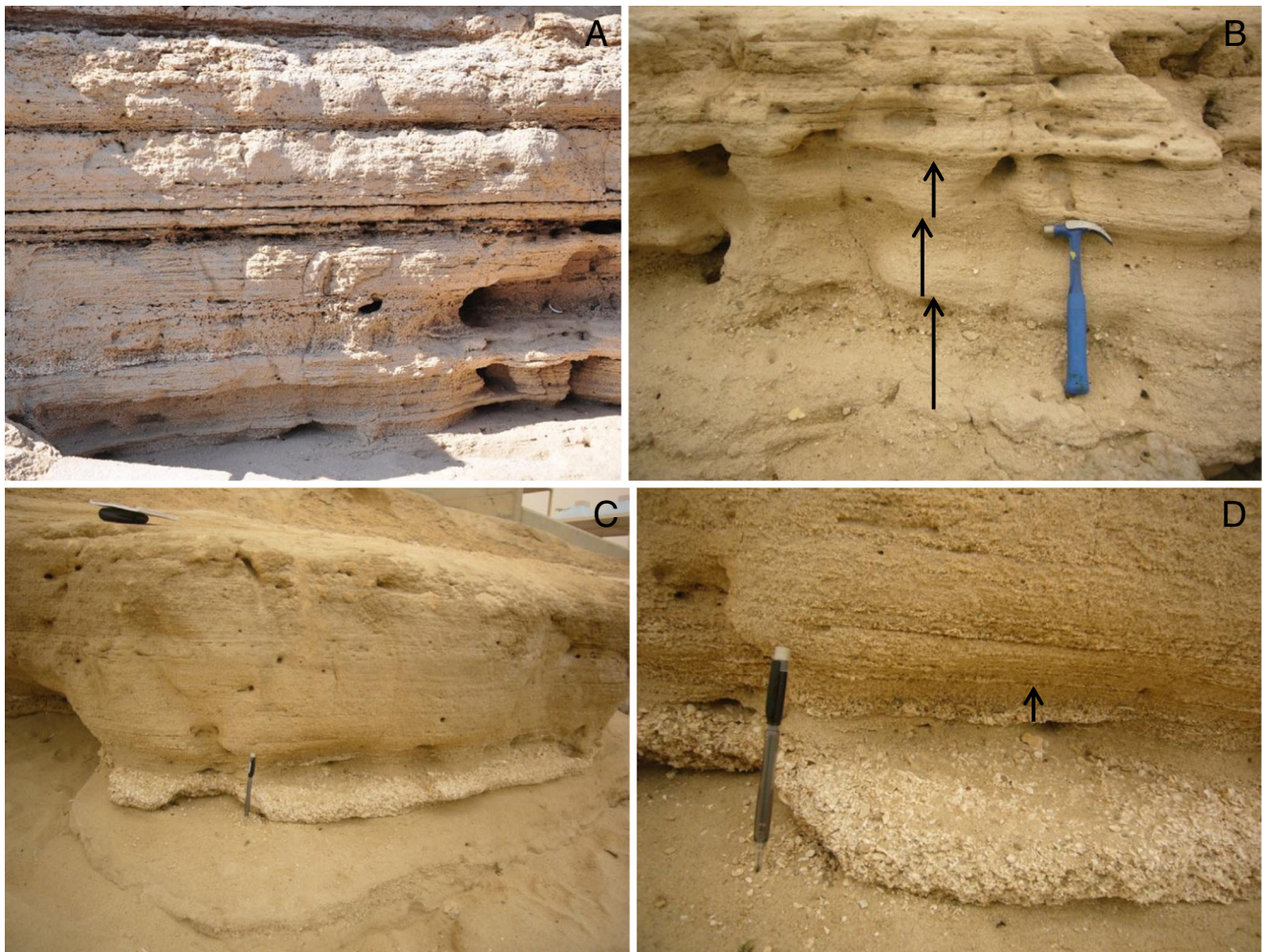**Fig. 4** Location of the Enjefa Beach

Fig. 5 Variations within the planar laminated facies. **a** Outcrop view of the planar laminated facies. **b** Coarsening upward beds marked by *arrows*. **c** Sharp-based coquina bed. **d** Close-up of the coquina bed which is internally cross-bedded and sharp-based normally graded lamination; an example is *arrowed*

2. Trough cross-bedded facies

Along strike, this facies occupies the middle part of the exposure area. It cuts into the planar laminated facies "a," which, as a result, is locally completely missing (Fig. 8). This facies is dominated by trough cross-bedded calcareous sandstone (Fig. 9). The dominant orientation of the

Fig. 6 Laterally pinching beds. Note the oppositely directed cross-beds above the pinch out bed

Fig. 7 Close-up of a part of the laterally pinching beds. Note the nicely lined fossil shells of gastropods and bivalves at base of the bed

Fig. 8 Along-strike contact between planar laminated facies (*left*) and trough cross-bedded facies (*right*). The latter facies cuts into the planar laminated facies. The *red dashed line* marks the southern edge of the channel

troughs is toward the northwest, with less common orientations toward east north. These cross-bedded laminae are sharply based and are internally normally graded (Fig. 9c) and are composed of well-rounded medium- to coarse-grained quartz grains, together with about 30 % of dark peloids and characterized by very high porosity (Fig. 10). The grains are coated with coarse equigranular rim calcite cement. Rare inclined burrows of Ophiomorpha (Fig. 9c) and bivalve shells are preserved at the base of beds (Fig. 9d).

This facies is interpreted the deposits of a tidal channel. The trough cross-beds were formed at the floor of the deeper part of the channel (cf. Moslow and Tye 1985; Boyd 2010) due to the development of mega-ripples. The dominant northwest (landward) current direction, which is oblique to the present shoreline, was thus the paleo-channel orientation. The local variations in current orientation are attributed to the sinuosity of the channel and as well as to ebb currents. Each lamina within the troughs was likely formed during relatively raised energy levels which waned quickly and as a result produced internal normal grading.

The coarse rim calcite cement around the grains was developed during early diagenesis, likely in the freshwater vadose zone diagenetic environments (Dr. Chris Kendall, personal communication 2011).

3. Planar wedge-shaped and ripple cross-bedded facies

This facies is about 1.5 m (5 ft) thick, laterally replacing the trough cross-bedded facies "b." It consists of well-sorted unimodal calcareous cross-bedded sandstone. The cross-beds are planar wedge-shaped with preserved megaripples (Figs. 11, 12, and 13). Although most of the cross-beds display current toward north, some southward-directed cross-bed sets are also present. Some individual sets of these cross-beds are up to 0.3 m (1 ft) thick. Locally, at the top of the megaripples, swollen lens-like sets are developed. This facies is composed of fine quartz grains along with 30–40 % dark peloids (Fig. 13). All grains of this facies are surrounded by equant calcite cement.

This facies was likely deposited in relatively shallow and possibly distal part of the tidal channel where energy levels were relatively less as compared to the middle part of the channel, where trough cross-stratified facies were deposited. Largely unidirectional and locally opposed cross-beds could result from wave action (De Raaf et al. 1977) and also due to the reversing tidal currents (Visser 1980; Dalrymple 2010). In the latter case, absence of typical tidal rhythmites could be attributed to the non-availability of suspended fine-grained sediments or to the higher current levels within the channel which would inhibit deposition of muddier sediments (cf. Moslow and Tye 1985). Furthermore, wave influence in the form of swollen lens-like sets at top of megaripples (De Raaf et al. 1977) may indicate relatively shallower water depths. Also, as seen in the trough cross-bedded facies b, the rim calcite cement likely developed during early freshwater vadose zone diagenesis.
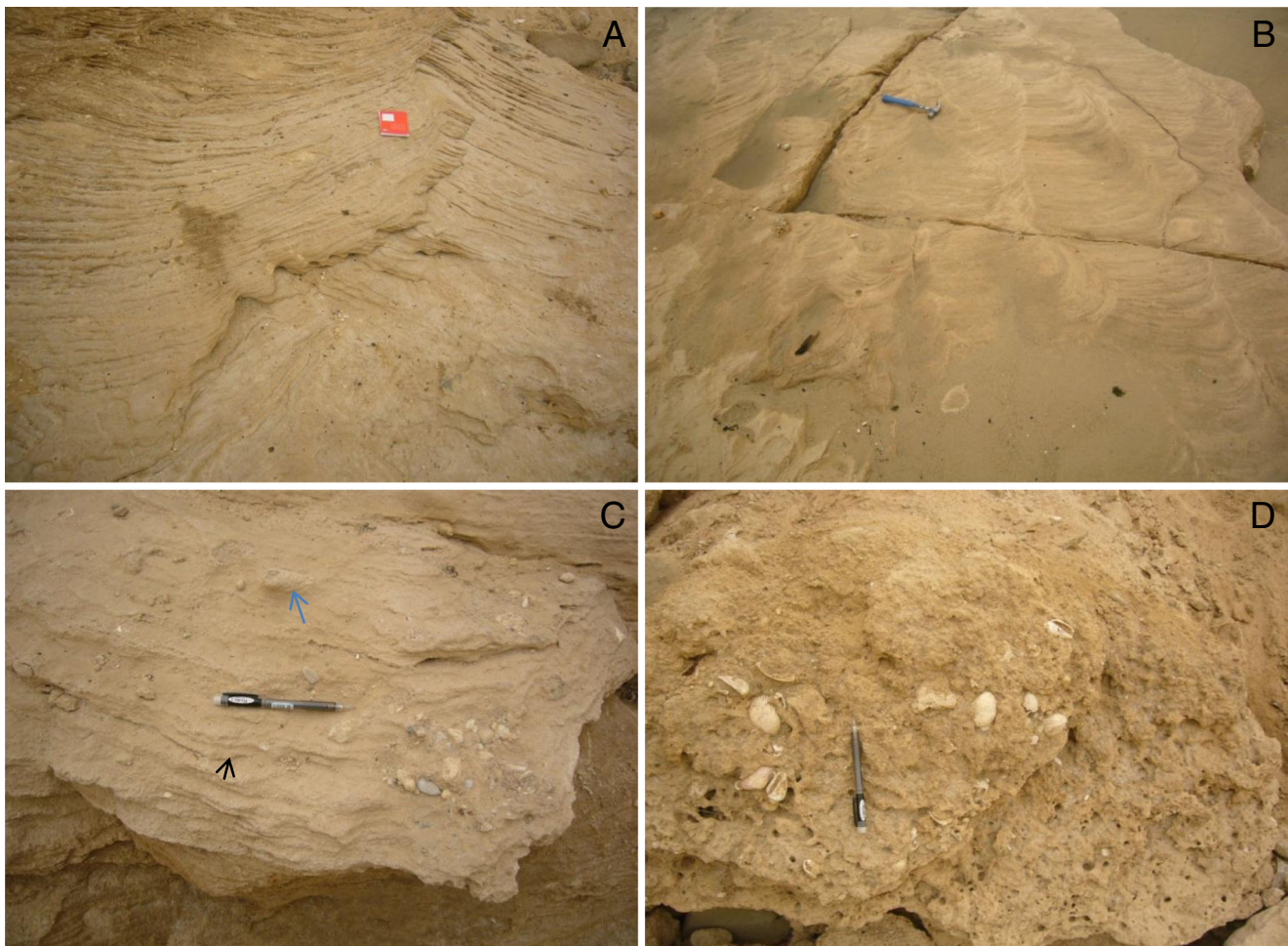
Fig. 9 Outcrop features in the trough cross-bedded facies. **a** Top and side view of large trough cross-beds. **b** Top view of trough cross-beds. **c** Top view of trough cross-beds showing normal grading within individual

lamina (*black arrow*) and rare inclined Ophiomorpha burrow (*blue arrow*). **d** Bivalve shells at base of one of the beds
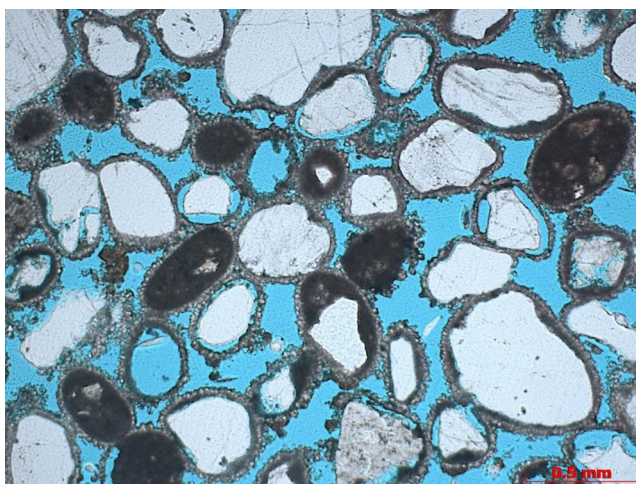
4. Bioturbated facies

This facies overlies the above-mentioned planar wedge-shaped cross-bedded facies (Figs. 14, 15, and 16) and consists of intensely burrowed sandstone. Primary

Fig. 10 Photomicrograph showing well-rounded quartz grains with dark color grains of peloids. The grains are coated with equigranular coarse carbonate rim cement. The dissolved grains and outer dissolved rims of quartz grains were possibly of aragonite composition which is removed by early diagenesis (Dr. Chris Kendall, personal communication). PP

Fig. 11 Outcrop photograph showing the planar wedge-shaped and ripple cross-bedded facies

Fig. 12 Close-up of a part of the above photograph showing mega-rippled beds

Fig. 14 Bioturbated facies showing intense burrowing. Locally sharp contact (hammer) with the underlying facies "c" is observable

depositional fabric is almost completely obliterated. A large network of burrows of Ophiomorpha and Parmaichnus is developed. Individual burrows are both horizontal and inclined to vertical and are up to 0.3 m (1 ft) in length (Fig. 15). Petrographic analysis of these burrow fills has shown predominance of sand-size peloids, which are well rounded and have internal micritized texture.

The stratigraphic position, as well as the presence of intense bioturbation and ophiomorpha burrows, suggests the deposition in protected coastal sand flat setting (cf. Carter 1978). Burrows were formed by shrimps and crabs with observed peloids as their fecal pellets. The Parmaichnus burrows (Pervesler and Uchman 2009) with turning chambers are thought to have been produced by shrimps in intertidal to subtidal environments (Dr. Dirk Knaust, personal communication 2011).
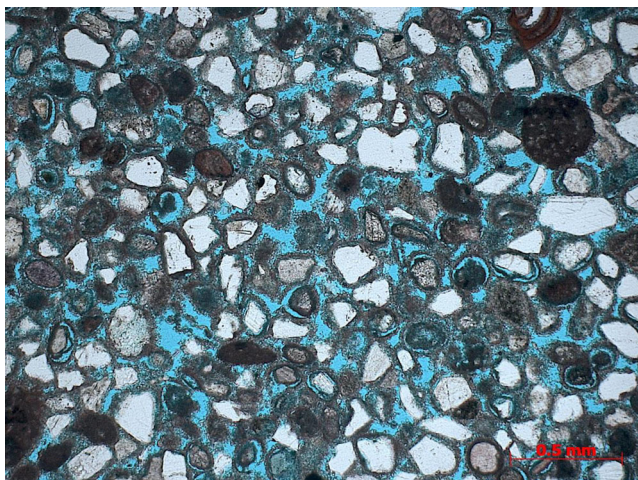
Facies stacking pattern

Walther's law of correlation of facies (Walther 1894 in Middleton 1973) states that "only those facies which formed in geographically adjacent environments may become associated in vertical sequence. Thus, in vertical profile, we try to study the lateral facies relationships through time" (Figs. 17, 18, and 19). Along the strike planar laminated, trough cross-bedded and planar wedge-shaped cross-bedded facies lie laterally parallel to each other. However, in the far north side of the outcrop, the planar laminated facies underlies the planar wedge-shaped cross-bedded facies, which in turn is overlain by burrowed facies passing upward into continental alluvium (Fig. 17). This stacking pattern reflects seaward shift in facies and therefore progradation and consequently sea regression.

Fig. 13 Photomicrograph showing subangular to rounded quartz grains with dark color rounded peloids and subordinate feldspar grains with calcareous cement at the edges of grains. PP

Fig. 15 Close-up of the bioturbated facies showing inclined to vertical and horizontal networks of Ophiomorpha burrows
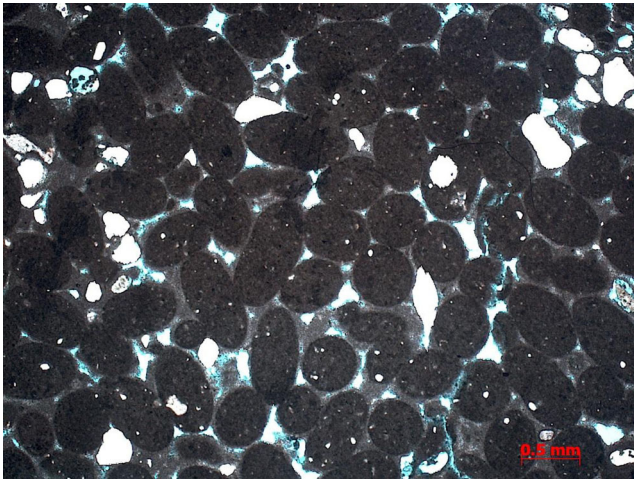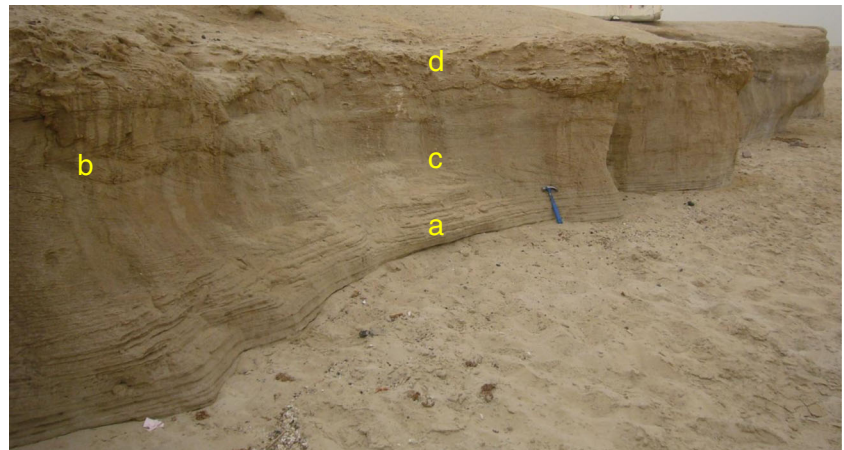
Fig. 16 Photomicrograph of a sample from within an Ophiomorpha burrow showing rounded peloids which internally consist of micritic texture. Subordinate white quartz grains are also present

The regressive conditions are further witnessed by the coarsening upward buildup within some individual beds in foreshore beach-deposited planar laminated facies "a." These exposures, therefore, not only represent shallow marine coastal foreshore beach, tidal channel, and sand flat subenvironments, but also record the sea regression during Holocene in Kuwait through their stacking pattern.

Age of the Enjefa Beach exposures

Radiocarbon ^{14}C age dating (Beta Analytic, Inc., Miami) was done on two samples, collected from the upper part of the exposure from the planar laminated facies "a." Sample EB-S1 was broken from a protruding layer edge (Figs. 20 and 21). It consisted of small-scale barnacles and likely other fossil shells as well. Sample EB-S2 consisted of large fossil shells, mostly of gastropods and bivalves (Fig. 21).
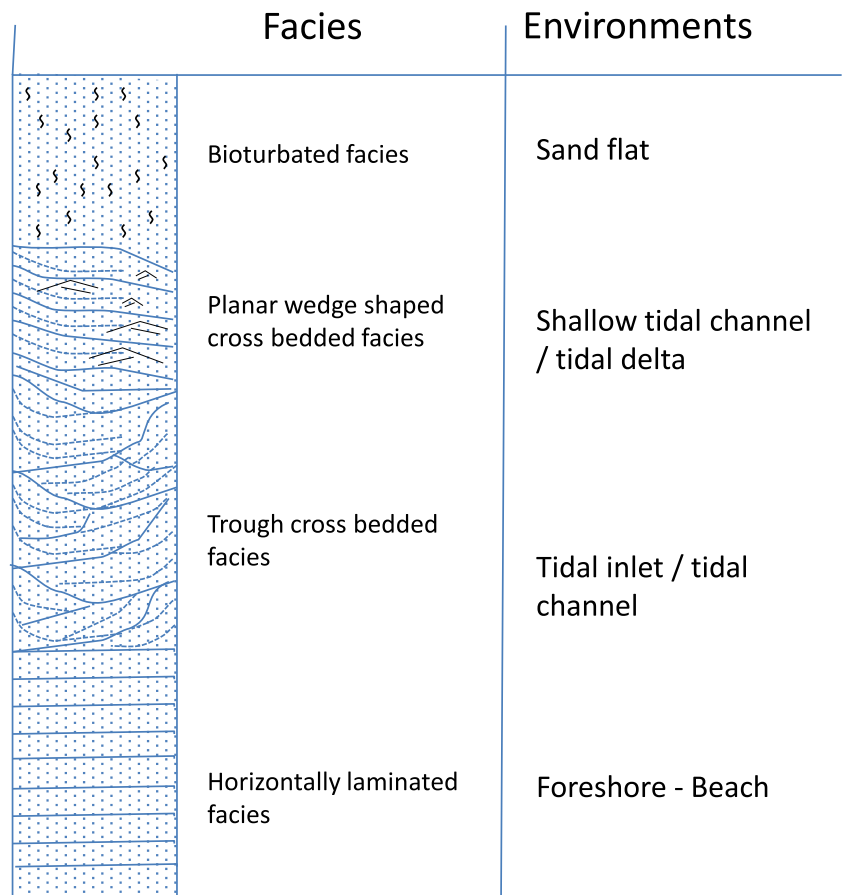
The age range from these two samples (Table 1) is close to each other and is considered reliable. Furthermore, the samples were collected from near the top of the exposures which suggest that

– In northern Arabian Gulf, the final phase of relative sea level fall likely occurred around circa 1,800 years BP which is similar to the conclusion reached at from eastern Australia by Lewis et al. (2008).

Sedimentological evidence for the late Holocene sea level change: a discussion

The mere exposure of the Holocene coastal shallow marine rocks at Enjefa Beach is evidence that the relative sea level once stood higher than the present day at this location. The facies stacking in the Enjefa Beach exposures from bottom to top is planar laminated facies "a" of foreshore beach origin which has been cut into and overlain by tidal channel trough cross-bedded facies b and planar wedge-shaped and ripple cross-bedded facies "c." These are overlain by sand flat bioturbated facies "d" and above, which represents present-day human infill with an unconformity in between. This clearly portrays a seaward shift in facies and, therefore, progradation during deposition of these sediments. Some of the individual beds in the planar laminated foreshore facies "a" display coarsening upward trend. These were developed by stacking of the beach face sediments. The basal fine sediments, which originated seaward of the coarser beach waterline mark, suggest progradation. The comparison of live barnacles (Fig. 22) inhabiting shallow shoreline setting (Pirazzoli 1991) with their fossil counterparts at the Enjefa Beach (Fig. 23) also suggests progradation and retreat of shoreline during deposition of these facies.

Fig. 17 Photograph from the northern side of the exposure showing vertical stacking of facies "a" to "d." Facies "b" laterally gives way to facies "c." Burrowed facies d has sharp and undulatory lower contact, and it merges up into the alluvium and present-day rubble

Fig. 18 Schematic vertical stacking of facies "a" to "d"

Facies	Environments
Bioturbated facies	Sand flat
Planar wedge shaped cross bedded facies	Shallow tidal channel / tidal delta
Trough cross bedded facies	Tidal inlet / tidal channel
Horizontally laminated facies	Foreshore - Beach

In addition to the glacio-hydro-isostatic adjustment (Lambeck, et al. 1995), ongoing tectonic activity in the Arabian Plate is likely playing an important role in the relative sea level changes in the Gulf. The Oligocene (post-Dammam) to present-day spike in the structural growth chart (Fig. 24) is related to the Neo-Tethyan closure, a continent to continent collision creating the Zagros event and the opening of the Red Sea. Uplift along the margin of the Red Sea and the northeastward movement of the Arabian Plate under the Zagros fold belt are creating intraplate stresses. There is present-day NE–SW compression within Kuwait, and possibly in other parts of the Arabian Plate, resulting in coastal and interior areas that are experiencing uplift and related local erosion.

Lines of evidence for Late Cenozoic structuring in Kuwait are documented and presented by Al-Ajmi et al. (2008). In this study, Al-Ajmi et al. (2008) have shown the recent uplift in southern Kuwait around the vicinity of the Greater Burgan structure, which has led to the successively northward shifting of the Dibdibba drainage during the Holocene (Fig. 25). The Dibdibba fan gravels in north Kuwait have been observed lying ca. 20 m higher than in the adjacent parts of the fan near Bahra area (Al-Ajmi et al. 2008), suggesting tremendous growth in structuring in Holocene times in Kuwait. This neotectonic phenomenon may have some role in the local sea level drop and exposure of the Holocene rocks along the Enjefa Beach.

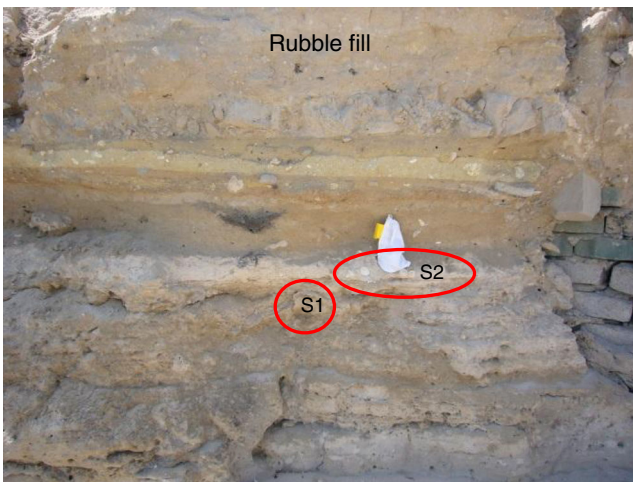**Fig. 19** Schematic representation of paleo-environments for the facies at Enjefa Beach
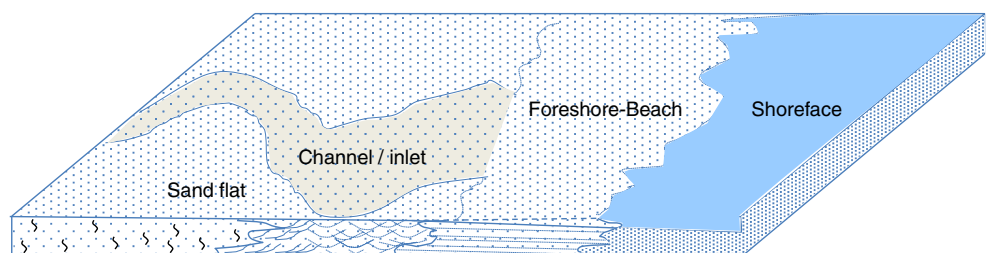
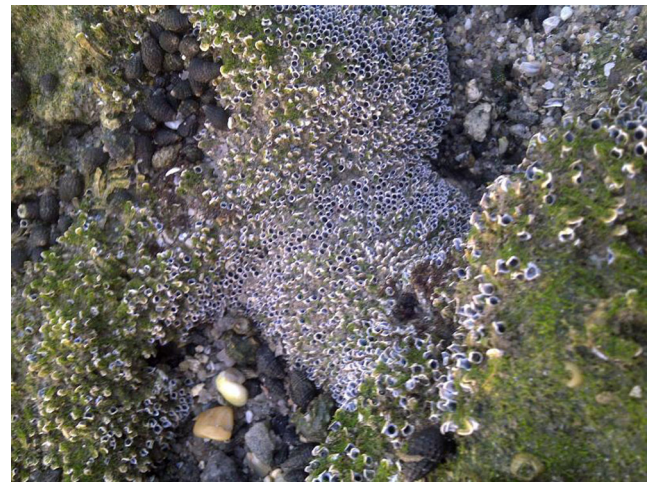**Fig. 20** Location of sample S1 and S2 from south side of the Enjefa Beach exposures

Fig. 22 Live encrusting barnacles, gastropods (dark color), and thin layer of green algae in the intertidal area at Enjefa Beach
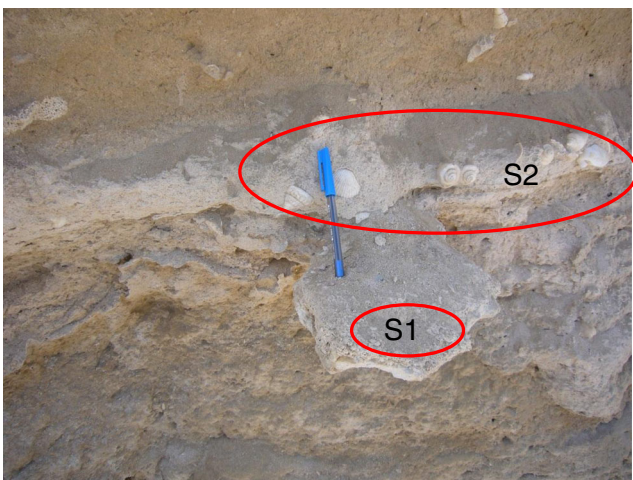

Fig. 21 Close-up of the above photograph showing location of sample S1 and S2. In the *upper circle*, large embedded mainly gastropod shells used for age dating are visible

Fig. 23 Fossil barnacles within Enjefa Beach exposure indicating one time sea level stood higher than the present level

Table 1 Age of the selected samples from the Enjefa Beach exposures

Sample name	Measured radiocarbon age (years BP)	^{13}C/^{12}C ratio	Conventional radiocarbon age[a] (years BP)
EB-S1	1,840±30	+0.5 o/oo	2,260±30
EB-S2	2,730±30	+1.3 o/oo	3,160±30

[a] The conventional radiocarbon age represents the measured radiocarbon age corrected for isotopic fractionation, calculated using the delta ^{13}C
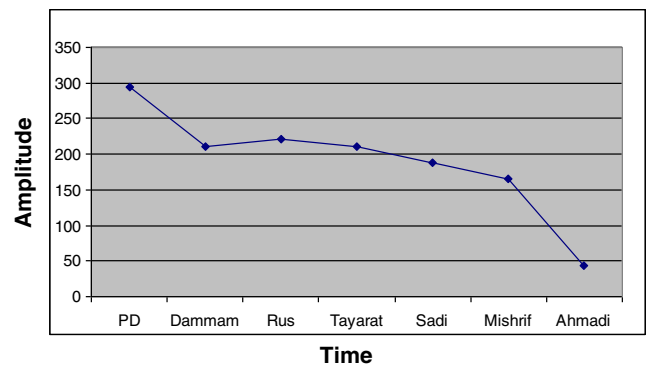

Fig. 24 Structural growth chart in Kuwait *Ahmadi* Cenomanian, *Mishrif* Turonian, *Sadi* Santonian, *Tayarat* Maastrichtian, *Rus* Ypresian, *Dammam* Lutetian-Bartonian, *PD* present day
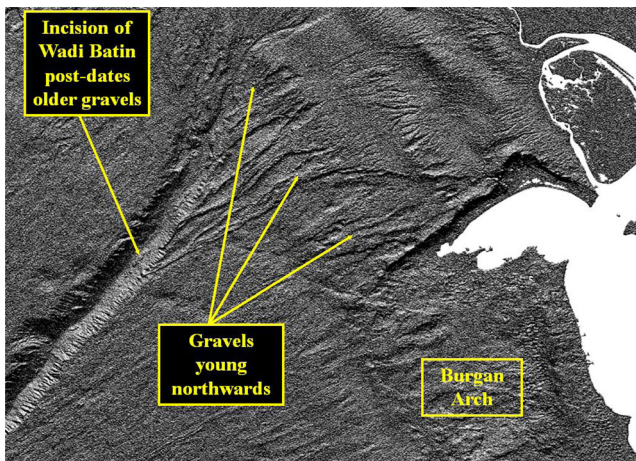
Fig. 25 Successive northward shift in the drainage of the Dibdibba Basin shown on SRTM map (Al-Ajmi et al. 2008)

Fig. 26 Terrace (ridge) and runnel physiography in the intertidal area at Enjefa beach developed due to the active present-day erosion by currents and waves

Fig. 27 Close-up showing eroded Holocene rock blocks in the runnel area

Present-day scenario

At the Enjefa Beach, the lower part of the Holocene exposure is inundated by seawater and now makes part of the intertidal zone. Due to the erosional activity of the waves and currents, this part of the Holocene rocks has developed into a shore parallel ridge and runnel physiography (Figs. 26 and 27). Broken and eroded blocks of these rocks are seen lying in adjacent locations. Is it due to some local phenomenon or do these observations suggest present-day renewed sea transgression and drowning of the coastal area? More data from a wider spectrum are required to reach a viable conclusion.

Conclusions

The generalized conclusions of this study are as follows:

- The exposures at Enjefa Beach display classical succession of foreshore to beach, tidal channel, and sand flat facies and are a good fossil example of a sandy shoreline dissected by a tidal channel.
- The studied exposures, and equivalent exposures along the coast of the Arabian Gulf, were deposited during relative regressive phase(s), within the overall transgression during Holocene time. Final phase of relative sea level drop likely occurred around 1,800 years BP.
- Local and regional Arabian Plate tectonics could have contributed in developing the mid to late Holocene relative sea level drop.
- More data is required to confirm the present state of relative sea level in the coastal areas of Kuwait.

References

Aigner T (1985) Storm depositional systems. Lecture notes in Earth Sciences. Springer-Verlag, Berlin, 174 p

Al-Ajmi B, Al-Ashwak S, Tanoli S, Al-Kandari F, Al-Darmi A, Crossley R (2008) Late Cenozoic structuring in Kuwait: evidence and wider exploration and production implications. Geo 2008, Bahrain (abstract)

Al-Zamel AZ (1983). Geology and oceanography of recent sediments of Jazirat Bubiyan and Ras As-Sabiyah, Kuwait, Arabian Gulf. Unpublished Ph.D. Thesis, University of Sheffield

Anzidei M, Antonioli F, Benini A, Lambeck K, Sivan D, Serpelloni E, Stocchi P (2011) Sea level change and vertical land movements since the last two millennia along the coasts of southwestern Turkey and Israel. Quat Int 232(1):13–20

Aqrawi AAM (1995) Brackish-water and evaporitic Ca-Mg carbonates in Holocene lacustrine/deltaic deposits of southern Mesopotamia. J Geol Soc London 152:259–268

Aqrawi AAM (2001) Stratigraphic signatures of climatic change during the Holocene evolution of the Tigris-Euphrates delta, lower Mesopotamia. Glob Planet Chang 28:267–283

Boyd R (2010) Transgressive wave-dominated coasts. In: James NP, Dalrymple RW (eds) Facies models 4. GEOtext 6. Geo Ass Can, St. John's, pp 265–294

Carter CH (1978) A regressive barrier and barrier protected deposit: depositional environments and geographic setting of the late Tertiary Cohansey Sand. J Sediment Petrol 48(3):933–949

Catuneanu O, Abreu V, Bhattacharya JP, Blum MD, Dalrymple RW, Eriksson PG, Fielding CR, Fisher WL, Galloway WE, Gibling MR, Giles KA, Holbrook JM, Jordan R, Kendall CGSC, Macurda B, Martinsen OJ, Miall AD, Neal JE, Nummedal D, Pomar L, Possamentier HW, Pratt BR, Sarg JF, Shanley KW, Steel RJ, Strasser A, Tucker ME, Winker C (2009) Towards the standardization of sequence stratigraphy. Earth-Sci Rev 92:1–33

Dalrymple RW (2010) Tidal depositional systems. In: James NP, Dalrymple RW (eds) Facies models 4, GEOtext 6, Geol Ass Can, pp 201–231

De Raaf JFM, Boersma JR, Van Gelder A (1977) Wave generated structures and sequences from a shallow marine succession, Lower Carboniferous, County Cork, Ireland. Sedimentology 24:451–483

Evans G (2011) An historical review of the Quaternary sedimentology of the Gulf (Arabian/Persian Gulf) and its geological impact. In: Kendall C.G.St.C, Alsharhan AS (eds). Quaternary carbonate and evaporate sedimentary facies and their ancient analogues: a tribute to Douglas James Shearman. International Association of Sedimentologists Special Publication 43

Evans G, Kirkham A, Carter RA (2002) Quaternary development of the United Arab Emirates coast: new evidence from Marawash Island, Abu Dhabi. GeoArabia 7(3):441–458

Godwin H, Surggate RP, Wills EH (1958) Radiocarbon dating of the eustatic rise of ocean-level. Nature 181:1518–1519 http://www.globalwarmingart.com/wiki/File:Holocene_Sea_Level_png

Kassler P (1973) The structural and geomorphic evolution of the Persian Gulf. In: Purser BH (ed) The Persian Gulf: Holocene carbonate sedimentation and diagenesis in a shallow epicontinental sea. Springer, New York, pp 11–32

Lambeck K (1996) Shoreline reconstructions for the Persian Gulf since the last glacial maximum. Earth Planet Sci Lett 142(1–2):43–57

Lambeck K, Johnston P, Smither C, Fleming K, Yokoyama Y (1995) Late Pleistocene and Holocene sea-level change: the Persian Gulf. Research School of Earth Sciences (RSES), Annual Report. The Australian National University, Canberra

Lambeck K, Purcell A, Dutton A (2011) The anatomy of interglacial sea levels: the relationship between sea levels and ice volumes during the Last Interglacial. Earth Planet Sci Lett 315–316:4–11

Lewis SE, Raphael AJ, Webster MJ, Shields GA (2008) Mid-late Holocene sea-level variability in eastern Australia. Terra Nova 20(1):74–81

McClure HA, Vita-Finzi C (1982) Holocene shorelines and tectonic movements in eastern Saudi Arabia. Tectonophysics 85(3–4):T37–T43

McIntosh JR (2005) Ancient Mesopotamia: new perspectives. ABC-CLIO, In. Santa Barbara, California, 395 p

Middleton GV (1973) Johannes Walther's Law of the correlation of facies. Geol Soc Am Bull 84:979–988

Moslow TF, Tye RS (1985) Recognition and characterization of Holocene tidal inlet sequences. Mar Geol 63:129–151

Nutzel W (1979) On the geographical position of as yet unexplored early Mesopotamian cultures: contribution to the theoretical archaeology. J Am Orient Soc 99(2):288–296

Pervesler P, Uchman A (2009) A new Y-shaped trace fossil attributed to upogebiid crustaceans from Early Pleistocene of Italy. Acta Palaeontol Pol 54:135–142

Pirazzoli PA (1991) World atlas of Holocene sea-level changes. Elsevier oceanography series, vol 58. Elsevier Science Publishers B.V, Amsterdam, 299 p

Reinson GE (1984) Barrier island and associated strand-plain systems. In: Walker RG (ed) Facies models, 2nd edn, Geoscience Canada Reprint Series 1, pp 119–140

Sarnthein M (1972) Sediments and history of the postglacial transgression in the Persian Gulf and Northwest Gulf of Oman. Mar Geol 12:245–266

SEMP Biot Report #422 (2007). Persian Gulf once dry, green, and inhabited by humans: implications. 4 p

Teller JT, Glennie KW, Lancaster N, Singhvi AK (2000) Calcareous dunes of the united Arab Emirates and Noah's flood: the postglacial reflooding of the Persian (Arabian) Gulf. Quat Int 68–71:297–308

Visser MJ (1980) Neap-spring cycles reflected in Holocene subtidal large-scale bedform deposits: a preliminary note. Geology 8:543–546

Williams AH, Walkden GM (2002) Late Quaternary highstand deposits of the southern Arabian Gulf: a record of sea-level and climate change. Geol Soc Lond Spec Publ 195:371–386